Hearing Research 273 (2011) 46–58

Contents lists available at ScienceDirect

Hearing Research

journal homepage: www.elsevier.com/locate/heares

Mechanics of the frog ear

Pim Van Dijk [a,b,*], Matthew J. Mason [c], Richard L.M. Schoffelen [a,b,d], Peter M. Narins [e], Sebastiaan W.F. Meenderink [f]

[a] Department of Otorhinolaryngology/Head and Neck Surgery, University Medical Center Groningen, The Netherlands
[b] School of Behavioral and Cognitive Neurosciences, Faculty of Medicine, University of Groningen, The Netherlands
[c] Department of Physiology, Development & Neuroscience, University of Cambridge, UK
[d] Department of Medical Technology and Clinical Physics, University Medical Center Utrecht, The Netherlands
[e] Departments of Physiological Science and Ecology & Evolutionary Biology, University of California Los Angeles, Los Angeles, CA, USA
[f] Department of Neuroscience, Erasmus MC, Rotterdam, The Netherlands

ARTICLE INFO

Article history:
Received 22 December 2009
Received in revised form
1 February 2010
Accepted 3 February 2010
Available online 10 February 2010

ABSTRACT

The frog inner ear contains three regions that are sensitive to airborne sound and which are functionally distinct. (1) The responses of nerve fibres innervating the low-frequency, rostral part of the amphibian papilla (AP) are complex. Electrical tuning of hair cells presumably contributes to the frequency selectivity of these responses. (2) The caudal part of the AP covers the mid-frequency portion of the frog's auditory range. It shares the ability to generate both evoked and spontaneous otoacoustic emissions with the mammalian cochlea and other vertebrate ears. (3) The basilar papilla functions mainly as a single auditory filter. Its simple anatomy and function provide a model system for testing hypotheses concerning emission generation. Group delays of stimulus-frequency otoacoustic emissions (SFOAEs) from the basilar papilla are accounted for by assuming that they result from forward and reverse transmission through the middle ear, a mechanical delay due to tectorial membrane filtering and a rapid forward and reverse propagation through the inner ear fluids, with negligible delay.

1. Introduction

From the time of their discovery, otoacoustic emissions have been considered a tool for noninvasive probing of inner ear mechanics (Kemp, 1978). However, the usefulness of OAEs in the study of cochlear mechanics has been hampered by a paradox. A proper interpretation of otoacoustic emissions depends on a rigorous knowledge of how the cochlea works; this includes the very inner ear mechanics that otoacoustic emission measurements are intended to elucidate. This situation recently led to a discussion of how otoacoustic emissions from the mammalian cochlea travel from the hair cells that generate them to the ear canal, where they are recorded. It has been proposed that this reverse propagation of otoacoustic emissions would depend on a "slow" backward travelling wave involving the basilar membrane, leading to a total emission round-trip delay of about twice the forward travelling wave delay (Shera and Guinan, 2003, see also Shera et al., 2008). In contrast, a direct and fast reverse propagation by compressive waves through the cochlear fluids has also been proposed, leading to an emission delay that approximately equals the forward travelling wave delay (Siegel et al., 2005; He et al., 2008). The complexity of cochlear structure and function in mammals has clearly contributed to the difficulties in determining the mechanisms involved in reverse otoacoustic emission propagation.

This review describes the mechanical properties of the frog inner ear and focuses on the various mechanical delays that contribute to the travel times of otoacoustic emissions in the frog ear. This ear contains two hearing organs, the amphibian and basilar papillae. As described below, the data available for the basilar papilla allow for a comprehensive description of transmission times in a system considered mechanically simpler than the mammalian cochlea: the frog ear contains no basilar membrane and there is no travelling wave supported by the tectorial membrane (TM) of the basilar papilla (Schoffelen et al., 2009; see below). The group delays of various sub-systems in the frog ear play a central role in this discussion. Group delay is a measure of the response delay of a device, and is proportional to the slope of the

Abbreviations: AP, amphibian papilla; BEF, best excitatory frequency; BP, basilar papilla; DPOAE, distortion-product otoacoustic emission; SFOAE, stimulus-frequency otoacoustic emission; SOAE, spontaneous otoacoustic emission; TM, tectorial membrane.

* Corresponding author. Address: Department of Otorhinolaryngology/Head and Neck Surgery, University Medical Center Gronigen, P.O. Box 30.001, 9700 RB Groningen, The Netherlands. Tel.: +31 50 3612550; fax: +31 50 3611698.
E-mail address: p.van.dijk@med.umcg.nl (P. Van Dijk).

0378-5955/$ – see front matter © 2010 Elsevier B.V. All rights reserved.
doi:10.1016/j.heares.2010.02.004

phase response curve; when plotting phase response curves as number of cycles vs. frequency, the delay equals the negative of the slope. For the frog, group delay estimates are available for the middle ear, the tectorial membrane of the basilar papilla, stimulus-frequency otoacoustic emissions, and auditory nerve fiber responses. We show that the total round-trip emission delay, to and from the frog basilar papilla, equals twice the middle ear delay plus the "filter delay" associated with the TM mechanical tuning. These results show that otoacoustic emissions generated within the frog inner ear can propagate to the outside world very rapidly, an observation consistent with the findings by Siegel et al. (2005) and He et al. (2008) for the mammalian cochlea.

2. The middle ear

The frog does not have an external ear comparable to that of most other terrestrial vertebrates. There is no pinna, and the vast majority of known species lack an ear canal. Although many species of frogs lack tympanic ears (see Mason, 2007 for a recent review), we shall restrict the following discussion to those species that do have them, concentrating on the frogs in the family Ranidae upon which most experimental auditory research has been performed. In members of this family, the tympanic membrane is flush with the surrounding skin and located caudal to the eye (Fig. 1 shows the major components of the middle and inner ears of a ranid frog). On the medial side of the membrane, a middle ear cavity is present. In general, this cavity is connected to the buccal cavity via a relatively wide and permanently open Eustachian tube (but see Gridi-Papp et al., 2008 for an exception). The tympanic membrane is coupled to the otic capsule via the extrastapes and the stapes (also referred to as extracolumella and columella). The cartilaginous extrastapes is loosely connected at its distal end to the center of the tympanic membrane, at its proximal end to the stapes shaft (pars media), and to the skull by means of a thin, flexible ascending process (see Fig. 1). The bony stapes shaft expands medially to become continuous with the cartilaginous footplate (pars interna). The footplate is contained within the rostral half of the oval window, the entrance to the inner ear. The caudal half of the oval window is occupied by the otic operculum, a typically cartilaginous element unique to amphibians. The operculum articulates with the stapes footplate, and is also connected to the shoulder girdle by means of the opercularis muscle.

The tympanic middle ear apparatus serves to transmit acoustic vibrations from the surrounding air to the inner ear fluids. When the tympanic membrane is pushed inwards, the extrastapes is also pushed inwards, rocking about the ascending process (Mason and Narins, 2002a); the downward motion of its proximal end in turn rotates the stapes, which pivots about its articulation with the inferior edge of the oval window, resulting in outward movement of the stapes footplate (Fig. 1b). The motions of the tympanic membrane and the stapes footplate are therefore 180° out of phase, at least at low frequencies (Jørgensen and Kanneworff, 1998; Mason and Narins, 2002a,b; see Fig. 2, red datapoints). When the footplate

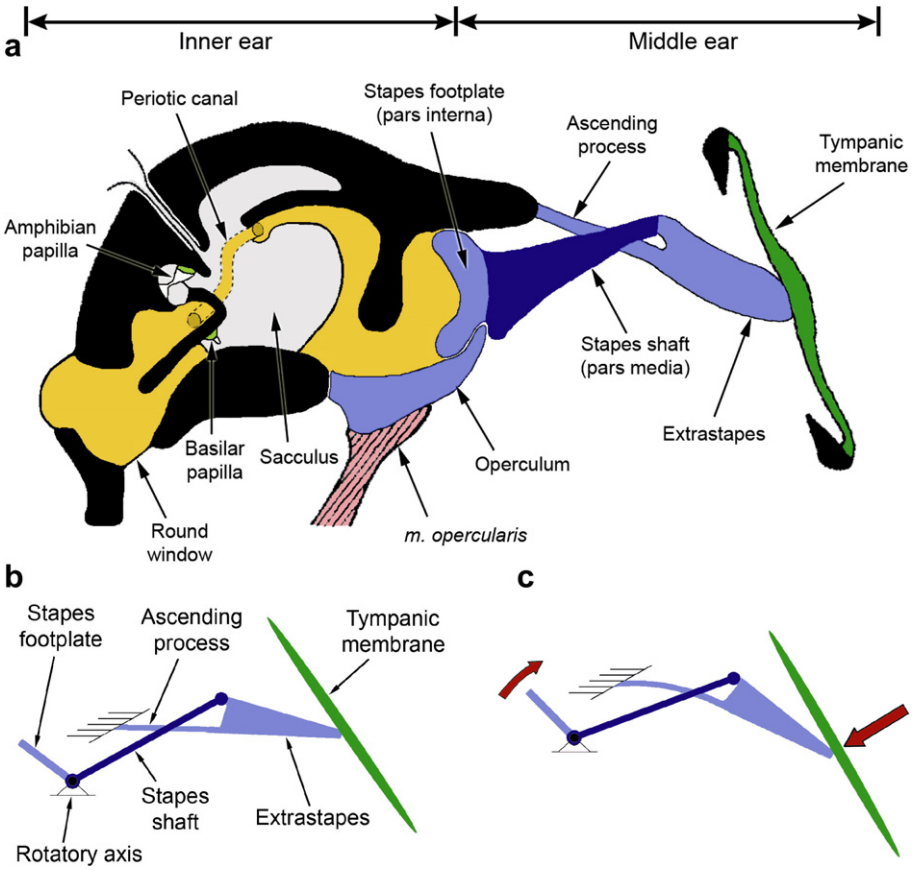

Fig. 1. Diagrammatic representations of (a) the middle and inner ear anatomy and (b and c) the lever mechanism of the middle ear, in a generalized ranid frog. In part (a), the inner ear is shown in frontal section, adapted from the schematic representation of Wever (1973). The stapes and extrastapes are drawn after Mason and Narins (2002a), and are shown, for the purposes of clarity, in transverse section (these structures are therefore shown twisted by 90° relative to the inner ear). Parts b and c (taken from Mason, 2007) represent the movements of the middle ear structures in response to movement of the tympanic membrane, according to the interpretation of Mason and Narins (2002a). The stapes (shaft and footplate) rocks about its rotatory axis, located ventrolateral to the footplate. Movement of the footplate relative to the tympanic membrane is reduced by flexion of the articulation between extrastapes and stapes shaft. The flexible ascending process is a vital part of this ossicular mechanism. [The inner ear and tympanic membrane in part (a) were reproduced from Wever (1973) with kind permission of John Wiley and Sons. Part (b) and (c) were reproduced from Mason (2007) with kind permission of Springer Science + Business Media.]

moves outward, a caudally-directed flange also lifts the operculum, which pivots around its attachment to the superior edge of the oval window. The operculum and the footplate move in phase over a large portion of the auditory sensitivity range of the frog ear (Mason and Narins, 2002b).

The function of the operculum is still debated (Mason, 2007). When the opercularis muscle contracts, one would imagine that it would lift the operculum out of the oval window. This could provide a bypass to attenuate sound transmission from the stapes into the inner ear. However, the opercularis muscle is a tonic muscle, specialized to contract relatively slowly and to maintain its tension for a prolonged time interval (Becker and Lombard, 1977). Hence, it is unlikely that the operculum and its associated muscle play a role in the protection against sudden loud sounds (Hetherington, 1994). Alternative suggestions have included a role for the opercularis system in the detection of ground vibrations (Hetherington, 1985, 1987, 1988; Hetherington et al., 1986), or in protecting the ear against the middle ear pressures that build up during vocalization and breathing (Mason and Narins, 2002b). Alternatively, it may serve as a release point of acoustic pressure in the inner ear. In other words, the opercularis system may have a function similar to that of the round window.

The lever action of the middle ear can be quantified as the ratio between the tympanic membrane velocity and the footplate velocity. In female bullfrogs (*Rana catesbeiana*), this ratio averages 17.0 dB at frequencies below 2 kHz (Mason and Narins, 2002a). Pressure amplification is provided not just by the ossicular lever, but presumably also by the ratio of the tympanic membrane area to stapes footplate area, which is around 20 (i.e. 26 dB) in female bullfrogs (Mason et al., 2003). The tympanic membrane and stapes of the bullfrog can be driven by airborne sound over a wide frequency range, with a broad maximum in their velocity amplitudes between 0.4 and 2 kHz (Mason and Narins, 2002a). The responses of the same structures in the grass frog *Rana temporaria* are similar (Jørgensen and Kanneworff, 1998). The group delay of the middle ear of the female bullfrog was computed from the phase data in Fig. 2. The delay of the tympanic membrane relative to incident sound pressure is 0.53 ± 0.07 ms. Together with the group delay of the stapes footplate relative to the tympanic membrane (0.170 ± 0.005 ms), the total middle ear group delay sums to 0.70 ± 0.07 ms.

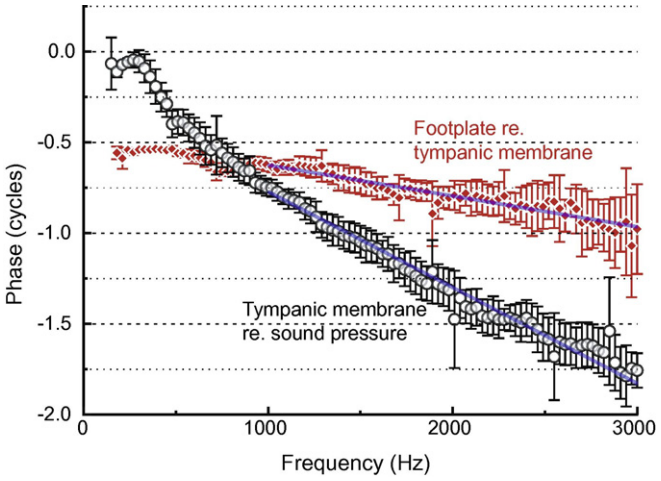

Fig. 2. Phase responses in the middle ear. The closed data points show the phase of footplate vibration relative to tympanic membrane vibration. These data points and their standard deviations were obtained by averaging the data representing female bullfrogs only from Fig. 4 in Mason and Narins (2002a). The open data points show the phase of the tympanic membrane vibration relative to sound pressure. The points were computed from data provided by Mason and Narins (unpublished), also for female bullfrogs. The group delay of the response was determined from the slope of a straight line fitted to the data points. The total middle ear group delay is $\tau_{ME} = 0.53\ (\pm 0.07) + 0.170\ (\pm 0.005) = 0.70\ (\pm 0.07)$ ms. Note that the location of the stapedial hinge point (see Fig. 1) accounts for the 180° phase difference between the footplate and the tympanic membrane at low-frequencies.

3. The inner ear

The ranid inner ear (see Fig. 1a) contains fluid, like the inner ear of all other vertebrates. The otic capsule has two windows, the oval window which is filled by the stapes footplate and operculum and the round window which, in ranids, is in the roof of the mouth and is covered by muscle tissue. Inspired by Lewis and Narins (1999), one might imagine a miniature scuba diver within the perilymph of the inner ear, who starts to swim away from the oval window. Passing from the lateral chamber, immediately behind the stapes and operculum, through a constriction into the inner ear proper, our scuba diver would see the otoconial mass of the sacculus at the other side of the membrane which separates the perilymph from the endolymph. He could swim through a narrow duct, the periotic canal, which surrounds the sacculus, whereupon he would pass the amphibian papilla and eventually end up in front of the round window. Looking back laterally in the direction of the sacculus, he would see two canals running close together and in parallel. These canals lead towards the amphibian and basilar papillae, respectively, the papillae being the end-organs which are dedicated to the detection of sound. The papillae would, however, be inaccessible to the diver, due to thin contact membranes separating the perilymph adjacent to the round window from the endolymph in the papillar recesses and the sacculus. The main function of these membranes appears to be the separation of endolymph and perlymph fluids, a role similar to that of Reissner's membrane in the mammalian cochlea, although they may also play a role in determining the frequency selectivity of the papillae (Purgue and Narins, 2000b).

3.1. Anatomy of the amphibian and basilar papillae

The amphibian papilla (AP) is on the dorsal wall of its recess; it consists of a patch of epithelium, covered in hair cells (see Fig. 3). The presence and size of the caudal extension of the papilla is species-dependent (Lewis, 1981): it is fully developed in ranids and hylids, providing the hair cell epithelium with its S-shaped appearance, but in some other frog species (e.g. *Bombina orientalis*, family Discoglossidae) the papilla lacks the extension and consists only of a triangular patch of hair cells corresponding to the rostral part of the ranid papilla.

The number of hair cells in the AP ranges from 676 to 1165 in ranid species (Fox, 1995). The hair cells are located on the stiff limbic wall of the papillar recess, which clearly contrasts with the anatomy in mammals, where the hair cells are mounted on a flexible basilar membrane. The stereovilli of the anuran hair cells are covered by a tectorial membrane and protrude into canals within it, the function of which are unknown (Wever, 1985; Lewis et al., 1992). The membrane has an acellular, gelatinous structure (Lewis and Leverenz, 1983). Towards the rostral end of the papilla, which faces the sacculus, the tectorial membrane is rather bulky, becoming thinner towards the caudal extension. Approximately halfway along the AP, a tectorial "curtain" spans the papillar recess. Interestingly, the orientation of the hair bundles is parallel to the S-shaped curvature in the rostral portion of the papilla. In contrast, their orientation is perpendicular to the curve in the portion caudal to the tectorial curtain, which is analogous to the hair cell orientation in the mammalian cochlea. The varying hair cell orientation pattern suggests complex vibration modes along the length of the AP tectorial membrane, but to date, no studies on these motions have been reported.

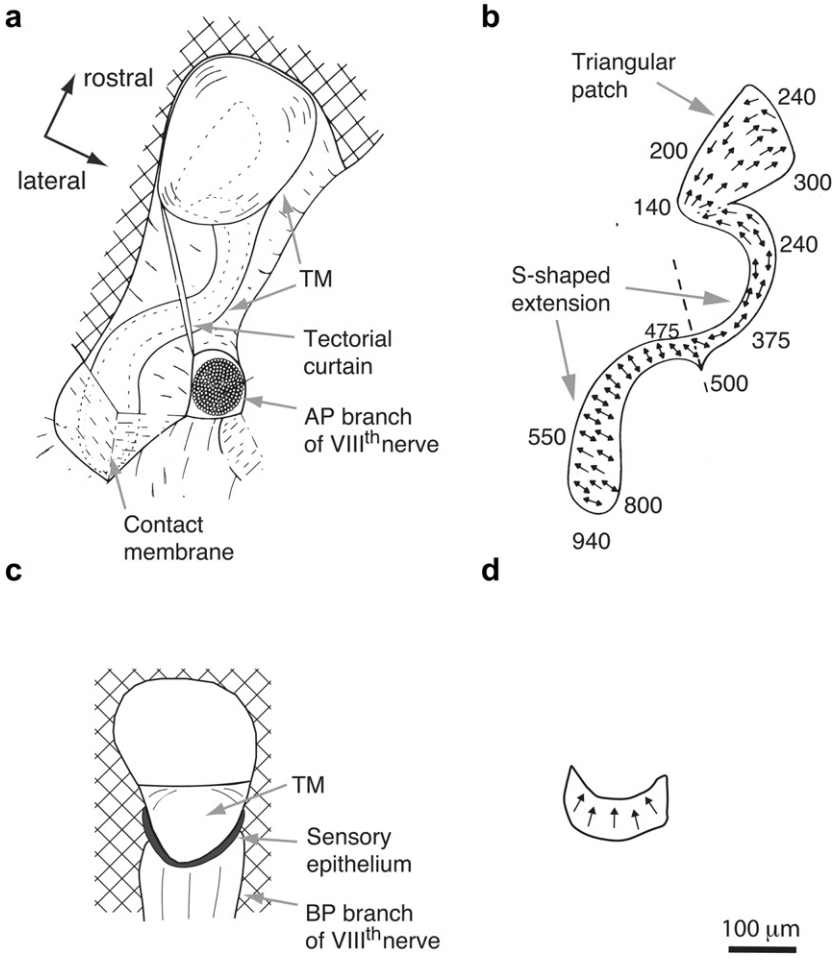

Fig. 3. Anatomy of the amphibian papilla (AP) and the basilar papilla (BP). (a) Ventral view of the AP (adapted from Lewis et al., 1982). The hair cell epithelium is outlined by thin, dashed curves. It is covered by the tectorial membrane (TM). A tectorial curtain blocks the recess of the AP. (b) Hair cell epithelium of the AP. The numbers indicate the approximate best excitatory frequency (BEF) in Hz of neurons that contact the corresponding location (*Rana catesbeiana*; adapted from Lewis et al., 1982). (c) Medial view of the BP, i.e. view of the BP from the round window (Schoffelen et al., 2009). The TM blocks approximately 1/3 of the papillar recess. (d) Lateral view of the hair cell epithelium of the BP, i.e. view from the sacculus. The epithelial surface is inclined by about 45° when viewed from the sacculus, so the lower portion of the figure is closer to the viewer than the upper portion (adapted from Schoffelen, 2009). The arrows on the epithelia in panels (b) and (d) indicate the excitatory direction of the hair cells' stereovilli. Double-headed arrows indicate regions of the epithelium where adjacent hair cells have opposing excitatory directions. The scale bar is approximate and applies to panels (a), (c) and (d); panel (b) has been slightly enlarged relative to the others. [Panel (a) and (b) were reproduced from Lewis et al. (1982) in a slightly adapted form with kind permissions of Springer Science + Business Media.]

The mechanism by which sound that enters the inner ear eventually stimulates the tectorial membrane of the amphibian papilla is also unknown. Possibly, vibrations travel from the oval window through the saccular space into the amphibian papilla (Wever, 1985; Purgue and Narins, 2000b). There, the vibrations could excite the tectorial membrane, for example by striking the tectorial curtain. After exciting the curtain, a sound wave could travel further through the contact membrane and towards the round window. A slit in the curtain could function as an acoustic bypass for high-intensity, low-frequency sound, which might otherwise damage the papilla (Lewis and Leverenz, 1983).

Compared to the amphibian papilla, the basilar papilla (BP) is simple in structure. It is positioned in a tube-like recess which runs from the contact membrane towards the saccular space. In the leopard frog (*Rana pipiens*), it can be visualized in an explanted otic capsule after removing a patch of bone at the round window (Schoffelen, 2009). The hair cell bodies are embedded on the medial wall of the tube, extending across approximately one third of its perimeter. The number of hair cells within the BP ranges from 51 to 99 among ranids in general (Fox, 1995). This number also varies within a species: numbers in *R. pipiens* range from 63 to 95 (Schoffelen, 2009). The tectorial membrane of the BP is semi-circular, the circular edge contacting the hair cell epithelium and the straight edge forming a relatively thick ribbon which spans the papillar recess (Lewis and Narins, 1999; Schoffelen, 2009). A number of hair bundles protrude into canals in the membrane, but since there are fewer canals than hair cells (Schoffelen, 2009), it is assumed that some hair bundles are free-standing (see also Lewis and Narins, 1999).

If our hypothetical scuba diver decided to penetrate through the BP contact membrane from the round window (perilymph) side, he would be able to touch the tectorial membrane and hair cells of the basilar papilla. Due to the only partial blockade of the basilar papillar recess by the tectorial membrane, the scuba diver could swim through to the sacculus by simply circumventing the membrane.

In ranids and hylids, the excitatory orientation of the hair cells' stereovilli is such that the tectorial membrane is expected to stimulate the BP hair cells by vibration away from the sacculus and towards the round window. An acoustic wave resulting from airborne sound stimulation must presumably enter the inner ear through the oval window, travel through the saccular space, enter the basilar papillar recess and exert a force on the tectorial membrane. Since the tectorial membrane of the papilla spans only about half the

cross-sectional area of the papillar recess, low frequencies will be shunted, while only higher frequencies may be assumed to cause an alternating pressure difference across the membrane.

3.2. Auditory nerve responses

Auditory neurons in the eighth cranial nerve exhibit a distinct frequency selectivity. This selectivity has been extensively characterized in a number of frog species by the measurements of neural tuning curves, also referred to as frequency threshold curves (Frishkopf and Goldstein, 1963; Frishkopf et al., 1968; Feng et al., 1975; Narins and Hillery, 1983; Benedix et al., 1994). The tuning curves are generally V-shaped. The frequency at which the lowest threshold is observed is referred to as the characteristic frequency (CF), or best excitatory frequency (BEF). The frequency width Δf at 10 dB above this minimum threshold has been used to characterize the frequency selectivity as a quality factor $Q_{10dB} = BEF/\Delta f$.

In the bullfrog, low-frequency neurons, with characteristic frequencies between 100 and about 500 Hz, innervate the rostral portion of the AP (Lewis et al., 1982). Mid-frequency neurons with BEFs between 500 and 1000 Hz innervate the caudal extension of the AP, while high-frequency neurons (BEF > 1000 Hz) connect to the basilar papilla (Lewis et al., 1982). The frequency ranges of these three neuronal groups differ between species. For example, in the Puerto Rican tree-frog, *Eleutherodactylus coqui* (Leptodactylidae), the distribution of BEFs (Fig. 1 in Narins and Capranica, 1980) suggests that these ranges are approximately 100–700 Hz, 700–1400 Hz and 2000–3800 Hz respectively, i.e. leaving a gap between the BEF values of the AP and the BP.

The tonotopy of the amphibian papilla was comprehensively described by Lewis et al. (1982), who traced auditory neurons to their peripheral origins. The characteristic frequencies of the auditory neurons that connect to the papilla systematically vary with the location of synaptic contact (see Fig. 3b). Rostral neurons are tuned to frequencies down to 100 Hz, while caudal neurons are tuned to frequencies up to 1000 Hz in the bullfrog. *In vitro* intracellular recordings from hair cells in the rostral portion and mid-section of the AP display electrical resonance in response to small current injections (*R. temporaria*: Pitchford and Ashmore, 1987; *R. pipiens*: Smotherman and Narins, 1999). In these experiments, no resonances above 375 Hz were described. Cells from the rostral portion and the mid-section of the AP in *R. temporaria* have resonance frequencies in the ranges 60–240 Hz and 210–330 Hz, respectively (Pitchford and Ashmore, 1987). Given that this frequency range is similar to the BEF range of nerve fibres innervating these regions (in *R. catesbeiana*), it is likely that the electrical resonances of the hair cells in the rostral portion of the AP contribute to the frequency selectivity of the auditory neurons that connect to these regions of the papilla. Since the upper limit of electrical resonance is 375 Hz, electrical resonances are presumably absent in caudal, higher-frequency hair cells.

In contrast to the AP, no tonotopic organisation has been identified in the BP of frogs. In *R. pipiens*, the vast majority of neurons have a nearly identical tuning-curve shape, suggesting that a single auditory filter dominates the response of the BP neurons (Ronken, 1991). The single-filter function has been confirmed by a comparison of tuning curves in *Rana esculenta* (Van Dijk et al., 1997a). Although most neurons have nearly identical tuning characteristics, a minority of neurons is tuned to a CF that is substantially higher than the predominant CF (see Fig. 12 in Van Dijk et al., 1997a). Possibly, these neurons connect to hair cells with free-standing hair bundles, which may have a higher resonant frequency due to the lack of a tectorial membrane mass load. Although the neurons in each individual frog display a uniform tuning-curve shape, the range of BEFs found in the basilar papillae of different individuals within a given species may span almost an octave (*R. pipiens*: Ronken, 1991; *E. coqui*: Narins and Capranica, 1980). This may relate to the finding of Meenderink et al., (2010), who showed that the variation of the tuning characteristics within a species is correlated with body size.

The quality factor Q_{10dB} typically ranges from 0.5 to 3.0 for neurons from both the AP and the BP (reviewed in Ronken, 1991). Some neurons in the AP have a quality factor up to 4.0 (Narins and Capranica, 1980). The threshold at BEF varies substantially across neurons. The least sensitive neurons have tuning-curve thresholds as high as 100 dB SPL (Shofner and Feng, 1981), while nerve fibers with the highest sensitivity have thresholds of about 30 dB SPL for the amphibian papilla and 40–50 dB SPL for the basilar papilla (*R. catesbeiana*: Shofner and Feng, 1981; *Hyla cinerea*: Ehret and Capranica, 1980; *R. pipiens*: Ronken, 1991). Thus, the lowest thresholds are found in the frequency range of the amphibian papilla, which is also the presumed site of generation of spontaneous otoacoustic emissions (see below).

Additional details about the tuning characteristics of auditory neurons can be obtained from Wiener kernel analysis. Wiener kernels can be obtained by cross correlation of a white noise acoustic stimulus and the corresponding neural response. The second-order Wiener kernel corresponds to a second-order correlation function between the acoustic noise input and the neural output (Schetzen, 1989; Van Dijk et al., 1994). This kernel may be used to describe a nonlinear system, such as the inner ear. It is analogous to the description of a linear system by an impulse response, which is also referred to as the first-order Wiener kernel. Like the amplitude of the Fourier spectrum of a linear impulse response, the two-dimensional Fourier transform of the second-order kernel describes the frequency selectivity of the neuron. In addition, components in the Fourier spectrum away from the diagonals in the frequency plane reflect the presence of nonlinear two-tone interactions.

One alternative interpretation of the Wiener kernels is based on singular value decomposition of the kernel matrix (Yamada and Lewis, 1999). This mathematical technique allows for a decomposition into excitatory and inhibitory kernels, which describe an increase and decrease, respectively, of the neuron's response to sound. Here we will limit our discussion to the opportunity to compute the group delay of the neuronal response from the highest-ranking singular component in the kernel. This component is interpreted as an impulse response that describes the most prominent component of the neuron's response. Hence, it describes both the frequency selectivity of the neuron and the group delay of the response. The amplitude spectrum of the highest singular vector provides an estimate of the BEF of the neuron.

Figs. 4 and 5 display second-order Wiener kernels of AP and BP neurons, respectively. A characteristic of the low-frequency neurons is the presence of off-diagonal components in the Fourier spectrum (Fig. 4b). In addition, low-frequency neurons exhibit two-tone suppression (Capranica and Moffat, 1980). The range of BEFs of neurons that exhibit two-tone suppression approximately corresponds to the frequency range for which off-diagonal components are present in the kernel (Van Dijk et al., 1997a). Also, body temperature appears to have a differential effect on the excitatory and inhibitory components of two-tone responses (Benedix et al., 1994) and on the diagonal and off-diagonal components in the Wiener kernel (Van Dijk et al., 1997b). Together, these results suggest that two-tone response attributes in the suppression experiments and off-diagonal components in the Wiener kernels may have a common physiological origin that differs from the main excitatory response of the neurons. Possibly, the two-tone interactions are related to the electrical resonances of hair cells, which are also confined to the low-frequency portion of the hearing range of the frog.

In the amphibian ear, neuronal responses of mid-frequency AP and high-frequency BP neurons are well described by a "sandwich

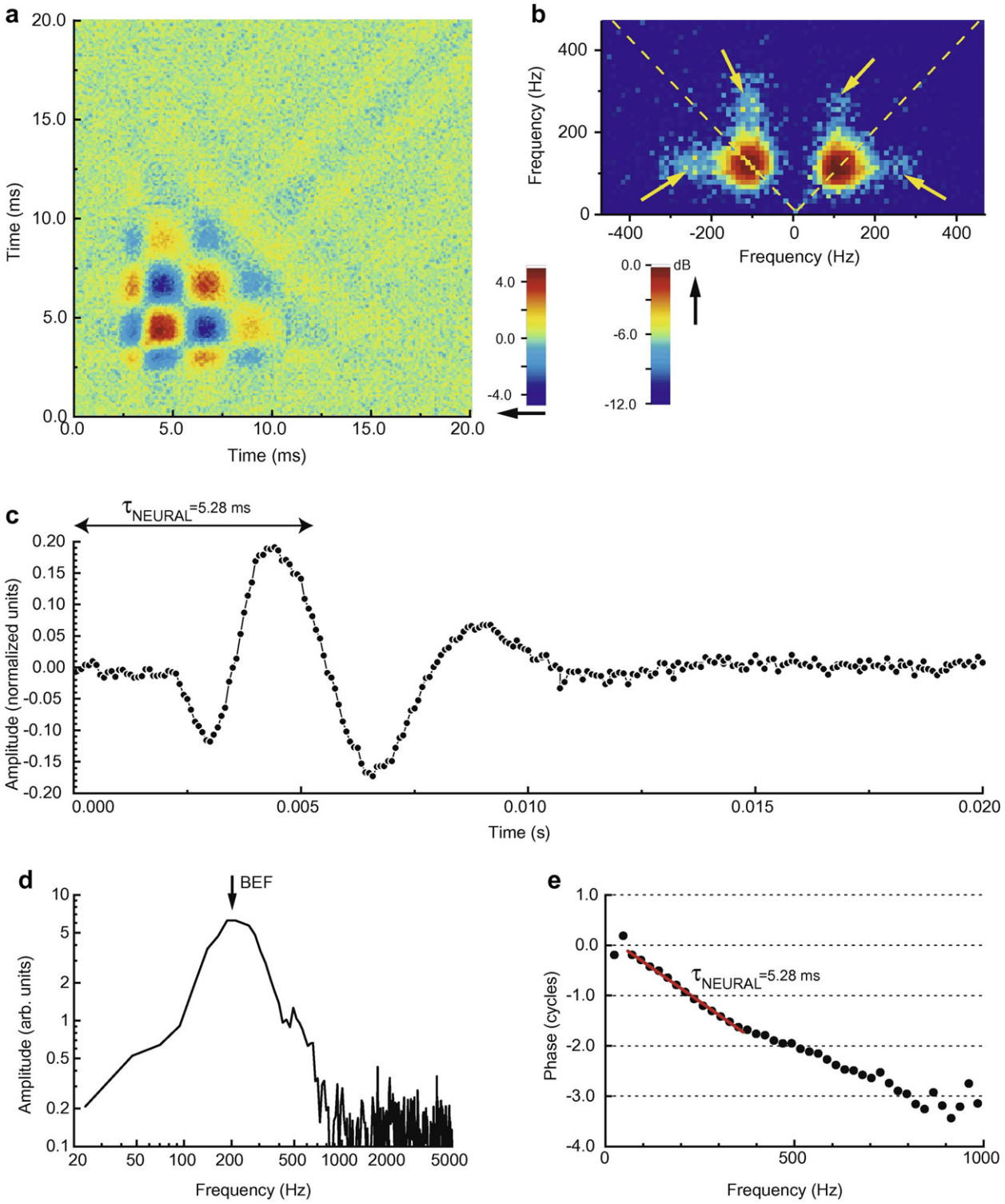

Fig. 4. Wiener kernel analysis of a low-frequency AP neuron in *Rana esculenta*, for which BEF = 200 Hz. (a) Second-order Wiener kernel. The color code is an arbitrary scale. (b) Two-dimensional Fourier transform of the kernel. The arrows indicate the off-diagonal components in the kernel. These components reflect two-tone interactions in the neuron's response. The color code is in dB re. the peak value. (c) First singular vector of the kernel. This vector is interpreted to reflect the most prominent component of the neural response. (d) Amplitude spectrum of the response in (c). (e) Phase spectrum of the response in (c). The negative of the slope of the phase curve equals the group delay of the response, i.e. $\tau_{NEURAL} = 5.28$ ms.

model", which consists of the cascade of a band-pass filter, a static nonlinearity, a low-pass filter and a spike generator (Korenberg, 1973; Van Dijk et al., 1994, 1997a). The sandwich model provides an intuitive interpretation of the Wiener kernels. The band-pass filter reflects the frequency selectivity of the auditory neuron. Across neurons, the band-pass filter's BEFs collectively make up the frog's mid- and high-frequency hearing range. Similarly, the range of quality factors Q_{10dB} for the band-pass filter corresponds to the range of quality factors that was reported for tuning curves (Van Dijk et al., 1997a). The nonlinear element relates to the hair cell

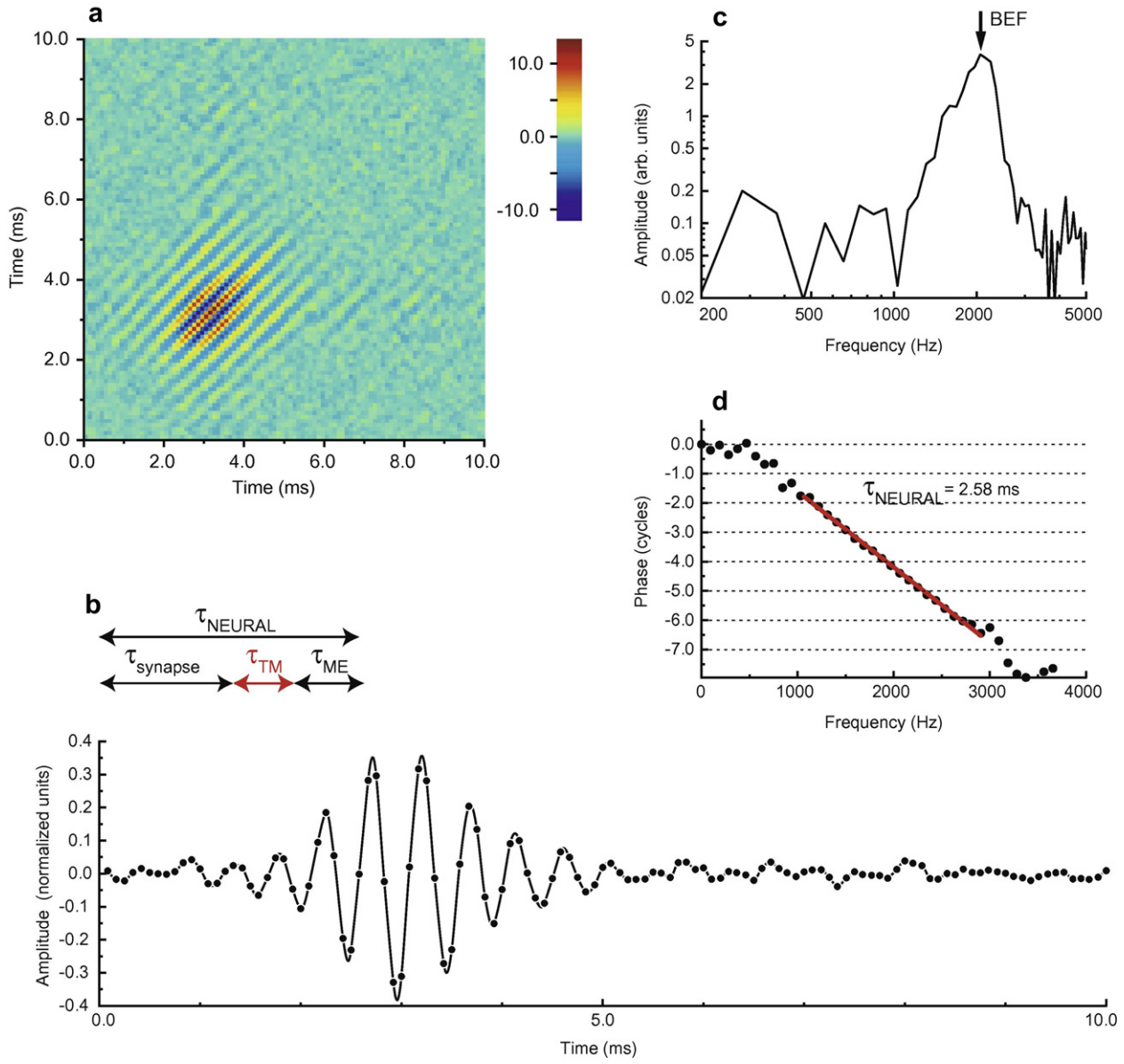

Fig. 5. Wiener kernel analysis of a BP neuron in *Rana esculenta*, for which BEF = 2062 Hz. (a) Second-order Wiener kernel. The color code is an arbitrary scale. (b) First singular vector of the kernel. This vector is interpreted as the impulse response of the auditory filter that provides the nerve with a frequency selective response. (c) Amplitude spectrum of the impulse response in (b). (d) Phase spectrum of the impulse response in (b). The group delay of the neural response is computed as the negative of the slope of the phase curve: $\tau_{NEURAL} = 2.58$ ms. The arrows in panel (b) illustrate that the neural group delay τ_{NEURAL} corresponds to the sum of the synaptic delay $\tau_{synapse}$, the mechanical filter delay of the tectorial membrane τ_{TM} and the middle ear delay τ_{ME}. See Table 2 for the numerical values of these three delays.

transduction mechanics. Finally, the low-pass filter reflects the electrical low-pass properties of the basolateral membrane of the hair cell, and the dynamics of the synapse. This filter limits the neuron's ability to phase lock to the acoustic stimulus. The low-pass filter has a cut-off frequency between about 180 and 300 Hz (Van Dijk et al., 1997a), which accounts for the decline of synchronization of neuronal responses with increasing tone frequency: Ronken (1990, *R. pipiens*) reported a 300-Hz cutoff for the 'synchronization-index filter function'.

The group delay plays an important role in the discussion of the inner-ear mechanisms that contribute to otoacoustic emissions and mechanical tuning (see below; for a corresponding discussion on the function of the mammalian cochlea, see e.g. Siegel et al., 2005 and Shera et al., 2008). Fig. 6 shows group delay estimates for *R. esculenta*, based on singular value decomposition of Wiener kernels (data from Van Dijk et al., 1997a,b) and from tone responses in *E. coqui* (Hillery and Narins, 1984)[1]. The group delays tend to decrease with increasing frequency. The relation between the neural group delay and BEF is remarkably similar to that in, for example, the chinchilla, *Chinchilla lanigera* (Recio-Spinoso et al., 2005, see Fig. 6). This similarity extends across a range of vertebrate species, as was also illustrated by Manley et al. (1990) for the squirrel monkey, the guinea pig, the starling, the bobtail lizard, and the caiman.

[1] Hillery and Narins (1984) estimated the middle ear and synaptic delay to be 2 ms in total. They subtracted this delay in the presentation of their Fig. 2C. In our Fig. 6, the 2-ms delay has been added again.

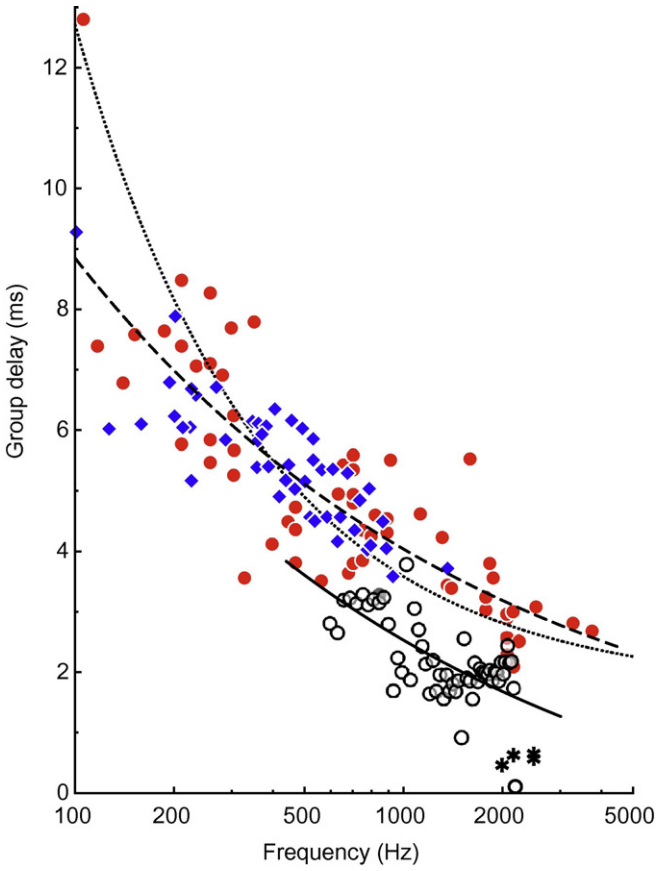

Fig. 6. Group delay of responses from the frog ear. Closed symbols: neural delays at the BEF. Open symbols: SFOAE delays. Closed circles: group delays obtained from the first singular vector of second-order Wiener kernels in *Rana esculenta* (reanalysis of the kernels in Van Dijk et al., 1997a,b). Closed diamonds: group delays from tone responses in *Eleutherodactylus coqui* (Hillery and Narins, 1984). Open circles: group delays of SFOAEs in *R. pipiens* in response to a low-level tone (68 dB SPL, Meenderink and Narins, 2006). Asterisk: group delay of the TM response to operculum stimulation in *R. pipiens* (Schoffelen et al., 2009; see also Fig. 7). The coarsely-dashed curve is a fit to the neural data points $\tau = 42.5 \times \mathrm{CF}^{-0.34}$. The solid curve is the same after subtraction of a constant delay equal to 1.5 ms. This delay was determined by a least-squares fit to the SFOAE data points. For comparison, the finely-dashed curve displays the fit to neural group delays in the chinchilla, as determined by Recio-Spinoso et al. (2005).

3.3. Otoacoustic emissions

The discovery of otoacoustic emissions in frogs (Palmer and Wilson, 1982) showed that active hearing mechanisms are not limited to mammalian cochleae. Spontaneous otoacoustic emissions (SOAEs) in frogs have levels up to 13 dB SPL (Van Dijk et al., 1989; reviewed in Manley and Van Dijk, 2008). The amplitude distribution of strong SOAE, which well exceeds the noise floor of the recording microphone, corresponds to that of a nearly sinusoidal tone (Van Dijk et al., 1989). SOAE frequencies are between 450 and 1350 Hz in ranids and between 650 and 1680 Hz in hylids (reviewed in Manley and Van Dijk, 2008). This is in the frogs' mid-frequency sensitivity ranges. Thus, these emissions presumably originate from the portion of the AP that is caudal to the tectorial curtain. A consistent finding is that SOAE frequencies appear slightly to exceed the upper BEF of AP neurons (Van Dijk et al., 1996; Van Dijk and Manley, 2001). The range of frequencies of SOAEs does not correlate with the BEFs of neurons from the basilar papilla (Van Dijk et al., 1989; Van Dijk and Manley, 2001; reviewed in Schoffelen et al., 2008). Hence, the basilar papilla presumably does not generate SOAEs. However, the AP and BP both appear to generate distortion-product otoacoustic emissions (DPOAEs; Van Dijk and Manley, 2001; Meenderink and Van Dijk, 2005) and stimulus-frequency otoacoustic emissions (SFOAEs; Meenderink and Narins, 2006). DPOAEs in the frequency range of the AP are more sensitive to hypoxia than those in the BP frequency range (Van Dijk et al., 2003). In addition, the DPOAEs that are generated in the AP by low-level stimuli are more sensitive to changes in body temperature than those generated in the BP (Meenderink and Van Dijk, 2006). This, together with the absence of SOAEs from the BP, suggests important differences between AP and BP physiology.

Although the peripheral origin of emissions seems to be clear from their frequencies, Meenderink and Narins (2007) show that suppression tuning curves of DPOAEs in the BP frequency range exhibit two minima. The lower-frequency minimum corresponds to the mid-frequency range of the AP while the deeper upper minimum is in the BP frequency range. This suggests that DPOAEs in the BP frequency range are dominated by a BP contribution, but a weaker AP component may be present as well.

Like DPOAEs, SFOAEs can be recorded for frequencies in both the AP and BP sensitivity range (Meenderink and Narins, 2006). The group delays of SFOAEs in the AP frequency range tend to decrease with increasing frequency. However, in the BP frequency range, the delay appears to be approximately constant: the average delay in the range 1900–2100 Hz is 2.1 (±0.2) ms (computed from data in Meenderink and Narins, 2006). In general, the SFOAE delay is about 1.5 ms shorter than that of the nerve response at a corresponding BEF.

3.4. Direct mechanical measurements of inner ear structures

Laser Doppler measurements of the vibration of the AP and the BP contact membranes in *R. catesbeiana* indicate that their responses correspond to the frequency ranges of the associated papillae (Purgue and Narins, 2000a). Based on these measurements and anatomical explorations of the bullfrog's inner ear, Purgue and Narins (2000b) constructed a model for the flow of vibrational energy through the frog's inner ear. In the model, three different pathways are identified along which acoustic signals may pass from the oval window to the round window. The signal is filtered according to the respective impedances of these pathways: (1) very low frequency sound and static pressures are shunted through the periotic canal and do not enter the endolymphatic space, (2) low-frequency sounds (100–1000 Hz) enter the endolymphatic space and pass through the AP recess, while (3) high-frequency sounds (>1000 Hz) also enter the endolymphatic space, but pass through the recess that holds the basilar papilla. In this model, the properties of the contact membranes provide the most significant contributions to the impedance of the respective pathways through the AP and the BP. Presumably, the impedance of the tectorial membranes, which are present in both the AP and BP pathways, contribute significantly to the total impedances of the respective inner sound paths through the endolymphatic space.

Ex-vivo measurements of the response of the BP's tectorial membrane (Schoffelen et al., 2009) indicate that the tectorial membrane is mechanically tuned to a frequency corresponding to the neural tuning frequency of that organ. The tuning sharpness of the TM is somewhat higher than that of the contact membrane in *R. catesbeiana* (Purgue and Narins, 2000a), and similar to that of the neural tuning curves in *R. pipiens* (Ronken, 1990, 1991). The group delay of the TM response relative to the operculum vibration ranges from 0.49 to 0.68 ms (see the asterisks in Fig. 6), with average $\tau_{TM} = 0.60$ (±0.08) ms.

For the AP, direct mechanical measurements have been limited to the measurements of the contact membrane (Purgue and Narins, 2000a). Although these measurements indicate the range of frequencies that pass through the AP recess, additional tuning

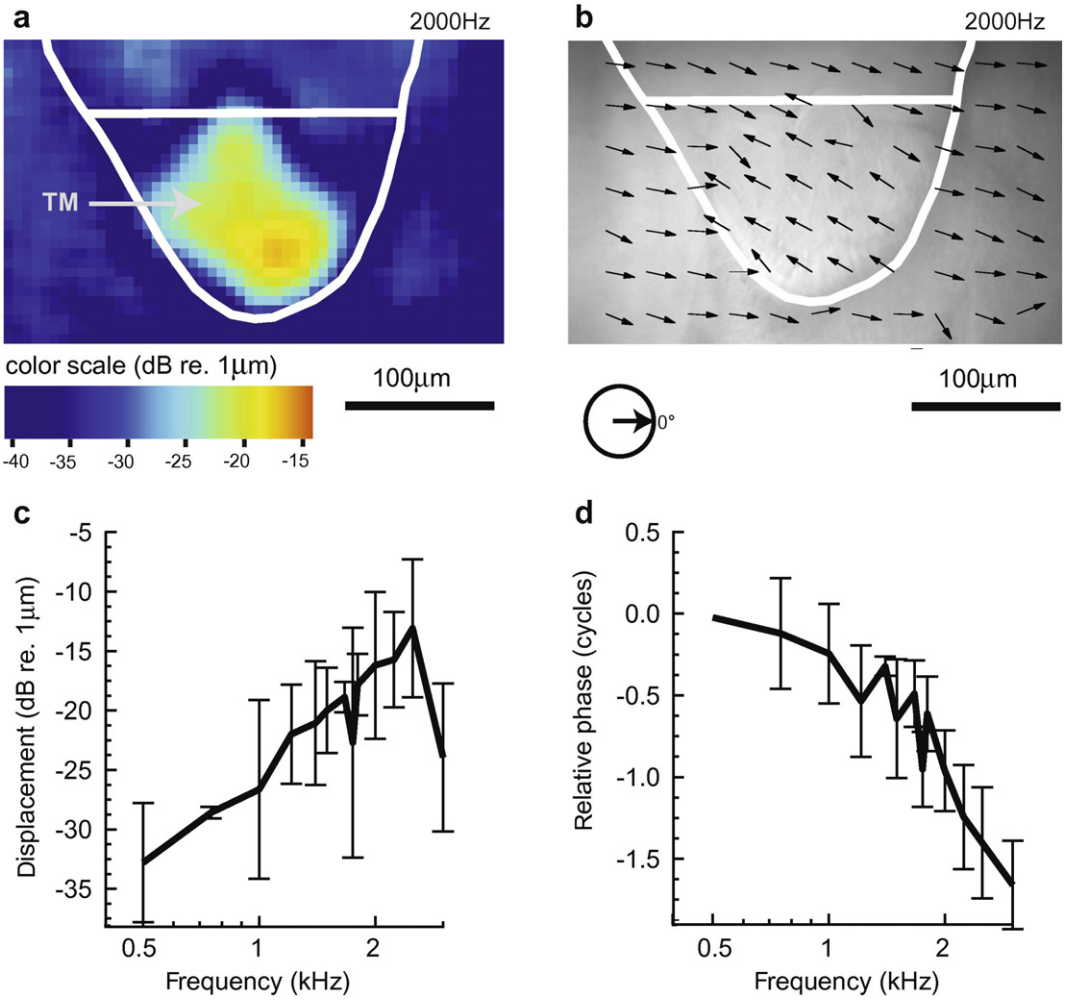

Fig. 7. Mechanical response of the TM to stimulation of the operculum. Refer to Fig. 3C for the anatomy of the BP. Panels (a) and (b) give an example of the response pattern at 2.0 kHz. The amplitude is color-coded in panel (a), the phase is superposed on a light-microscopy image of the BP in panel (b). Panels (c) and (d) show the averaged response of 5 preparations (from Schoffelen et al., 2009). The amplitude of the TM response is largest close to the hair cell epithelium (see panel a). The response phase is uniform across the TM (see panel b). Hence, there is no evidence of a travelling wave on the TM of the BP. The response is tuned to a frequency near 2 kHz (see panel c). Schoffelen et al. (2009) infered that the motion of the TM is along the surface of the hair cell epithelium in the excitatory direction of the hair bundles. Thus, the major component of the TM motion is in and out of the image planes in panels (a) and (b). [Reproduced from Schoffelen et al. (2009) with kind permission of the Association for Research in Otorhinolaryngology.]

mechanisms must be present to account for the tonotopy in the epithelium. Contributing factors are likely to include the mechanical properties of the tectorial membrane and the hair bundles, and, for the low-frequency region of the papilla, the electrical resonance properties of the hair cells (see above).

4. Discussion

An obvious functional similarity across the hearing organs of tetrapods is the sharply tuned, frequency-selective responses of auditory neurons. Interestingly, frequency selectivity arises despite the anatomical differences between vertebrate species. In frogs, the presence of at least two distinct hearing organs within one inner ear is remarkable. In addition, the amphibian papilla itself appears to include two functionally distinct regions. In the low-frequency rostral area of the papilla, electrical resonance of hair cells presumably contributes to the frequency selectivity, while such resonance has not been found in the caudal extension. In other words, the amphibian papilla itself may be considered to be a combination of two distinctly functioning auditory epithelia, a notion that is also consistent with the embryonic development of the papilla (Li and Lewis, 1974). The AP and the BP may therefore be viewed as three distinct functional systems: (1) the low-frequency rostral portion of the AP, (2) the mid-frequency caudal portion of the AP, and (3) the high-frequency BP (Feng et al., 1975).

Table 1 summarizes the key functional properties of the AP and the BP. There are some interesting correlations between the various properties. The presence of two-tone interactions in the auditory nerve response correlates with electrical resonance in the hair cells and with the absence of all types of otoacoustic emissions. Two-tone interactions are related to multiple tuning mechanisms (Benedix et al., 1994; Van Dijk et al., 1997a), which may suggest the interplay between the electrical tuning and possible mechanical tuning of the tectorial membrane.

It is tempting to imagine that the absence of otoacoustic emissions in the low-frequency range of the AP may be related to electrical resonance as a mechanism of frequency selectivity. However, there are alternative explanations for their absence. Perhaps the rather bulky tectorial membrane overlying the rostral portion of the amphibian papilla impedes reverse transmission and consequent emission of sound generated by the hair cells. Such a bulky TM is also present in the low-frequency portion of the inner ear in e.g. the bobtail lizard, which does not display spontaneous

Table 1
Characteristics of three distinct functional areas in the frog auditory epithelia.

	Amphibian papilla (AP)		Basilar papilla (BP)	References
Frequency range (in *Rana pipiens*)	Low 100–600 Hz	Mid 600–1250 Hz	High ~2000 Hz	
Anatomy				
Hair cell orientation re. tonotopic axis	Parallel	Perpendicular	N/A	Lewis (1981)
Physiology				
Tonotopy	Yes	Yes	Unknown*	
Electrical tuning	Yes (<375 Hz)	No	No	Pitchford and Ashmore (1987), Smotherman and Narins (1999, 2000)
Two-tone suppression	Yes	(Mostly) No	No	Frishkopf and Goldstein (1963), Benedix et al. (1994)
Off-diagonal components in the Wiener kernel	Yes	(Mostly) No	No	Van Dijk et al. (1994, 1997)
Mechanical tuning of membrane				
Basilar membrane	There is no basilar membrane			
Tectorial membrane	Unknown	Unknown	Yes	Schoffelen et al. (2009)
Contact membrane	Yes	Yes	Yes	Purgue and Narins (2000a)
Otoacoustic emissions				
Spontaneous OAEs	No	Yes	No	Van Dijk et al. (1989, 1996), Van Dijk and Manley (2001)
DPOAEs and SFOAEs	No	Yes	Yes	Van Dijk and Manley (2001), Meenderink and Van Dijk (2005), Meenderink and Narins (2006)

* The majority of BP neurons in an individual have nearly identical tuning properties. Exceptional neurons are tuned to a frequency that exceeds the dominant BEF by about 0.7–0.9 octave (Van Dijk et al., 1997a).

otoacoustic emission below 900 Hz (Köppl and Manley, 1993). In the frog and the lizard, the mechanical properties of the TM may be responsible for the lack of recordable emissions in the low-frequency portion of the papilla. In humans, otoacoustic emission frequencies typically exceed 500 Hz (Talmadge et al., 1993), which results from inefficient coupling between the inner and the outer ear at lower frequencies. A similarly inefficient coupling might explain the low-frequency boundary for anuran otoacoustic emissions.

The anatomical region responsible for transduction in the mid-frequency portion of the frog's auditory range, the caudal portion of the AP, is similar to the mammalian cochlea in that (1) it possesses a tonotopic organisation with the excitatory direction of the hair cells perpendicular to the tonotopic gradient (Lewis et al., 1982a); (2) the hair cells do not display electrical resonances (*in vitro*: Smotherman and Narins, 1999), and so the frequency selectivity of auditory neurons must be based on mechanical tuning of the tectorial membrane and hair cell stereovilli; (3) its frequency range overlaps with the range of spontaneous otoacoustic emissions; (4) otoacoustic emissions are vulnerable to physiological insults to the inner ear (Van Dijk et al., 2003). These similarities suggest that some common principle may underlie the function and tonotopic organisation of the cochlea and this portion of the amphibian papilla. Attempts to model the tonotopic organisation of the amphibian papilla have been unsuccessful (Lewis and Leverenz, 1983). Presumably, direct mechanical measurements of the tectorial membrane response will help to identify the properties of the tuning mechanism.

The basilar papilla, which covers the high-frequency portion of the auditory range in frogs, is a unique hearing organ in that (1) it does not appear to emit spontaneous otoacoustic emissions (Van Dijk et al., 1989; Van Dijk and Manley, 2001); (2) distortion-product otoacoustic emissions in the BP frequency range are relatively insensitive to ischemia (Van Dijk et al., 2003) and body temperature (Meenderink and Van Dijk, 2006), suggesting that their generation may be due to passive nonlinearities; (3) a tonotopic organisation is presumably absent (Ronken, 1990; Schoffelen et al., 2009), and finally, (4) the frequency selectivity of the BP can be essentially understood from the mechanical tuning of the TM (Schoffelen et al., 2009).

The relatively simple anatomical and functional organisation of the BP offers the opportunity to test some basic hypotheses about the transmission of acoustic stimuli to the hair cells, and the reverse transmission of otoacoustic emission from the hair cells to the external environment. If SFOAEs arise in the sensory hair cells after filtering of the corresponding stimulus by the tectorial membrane, and are transmitted back through the inner ear fluids to the outside world, the round-trip group delay can be estimated to correspond to the sum of the components of the round-trip transmission path. A diagrammatic representation of this path is shown in Fig. 8.

The group delay of SFOAEs in the BP of *R. pipiens* is $\tau_{SFOAE} = 2.0$ (± 0.1) ms (Meenderink and Narins, 2006; similar group delays also recorded by Bergevin et al., 2008). An SFOAE arises in response to a pure tone stimulus. Such a stimulus must travel through the middle ear and then through the inner ear fluids, whereupon it will excite the tectorial membrane. In the BP, the SFOAE presumably originate in the hair cells. Having been generated, the SFOAE travels a reverse pathway, from the BP to the tympanic membrane, via the middle-ear apparatus. Thus, the total group delay of the SFOAEs will be the sum of a number of contributions. The sound will travel twice through the middle ear, contributing to a delay $2 \times \tau_{ME} = 2 \times 0.70\ (\pm 0.07) = 1.40\ (\pm 0.14)$ ms (see Fig. 1), where we assumed the forward group delay to be equal to the reverse group delay (which is approximately true in the gerbil; Dong and Olson, 2006). In the inner ear, the travel time of the longitudinal waves through the fluid will be on the order of microseconds and will be neglected here. If we assume the hair cell nonlinearity, which results in the generation of the SFOAE, to be instantaneous, the group delay of this response will be identical to the group delay of the TM response. From the data presented by Schoffelen et al. (2009), we estimate the delay of the tectorial membrane relative to the operculum to be $\tau_{TM} = 0.60\ (\pm 0.08)$ ms. Thus, the total predicted group delay of the SFOAE is $\tau_{SFOAE,predicted} = 2 \times \tau_{ME} + \tau_{TM} = 2.00\ (\pm 0.16)$ ms, which closely corresponds to the measured value (Meenderink and Narins, 2006; see Table 2). This finding agrees with the view that SFOAEs are generated in a round-trip scheme as illustrated in Fig. 8.

In mammals, the mechanics are complicated by the presence of travelling waves involving the basilar membrane. In principle, waves could move both forward (from base to apex) and backward

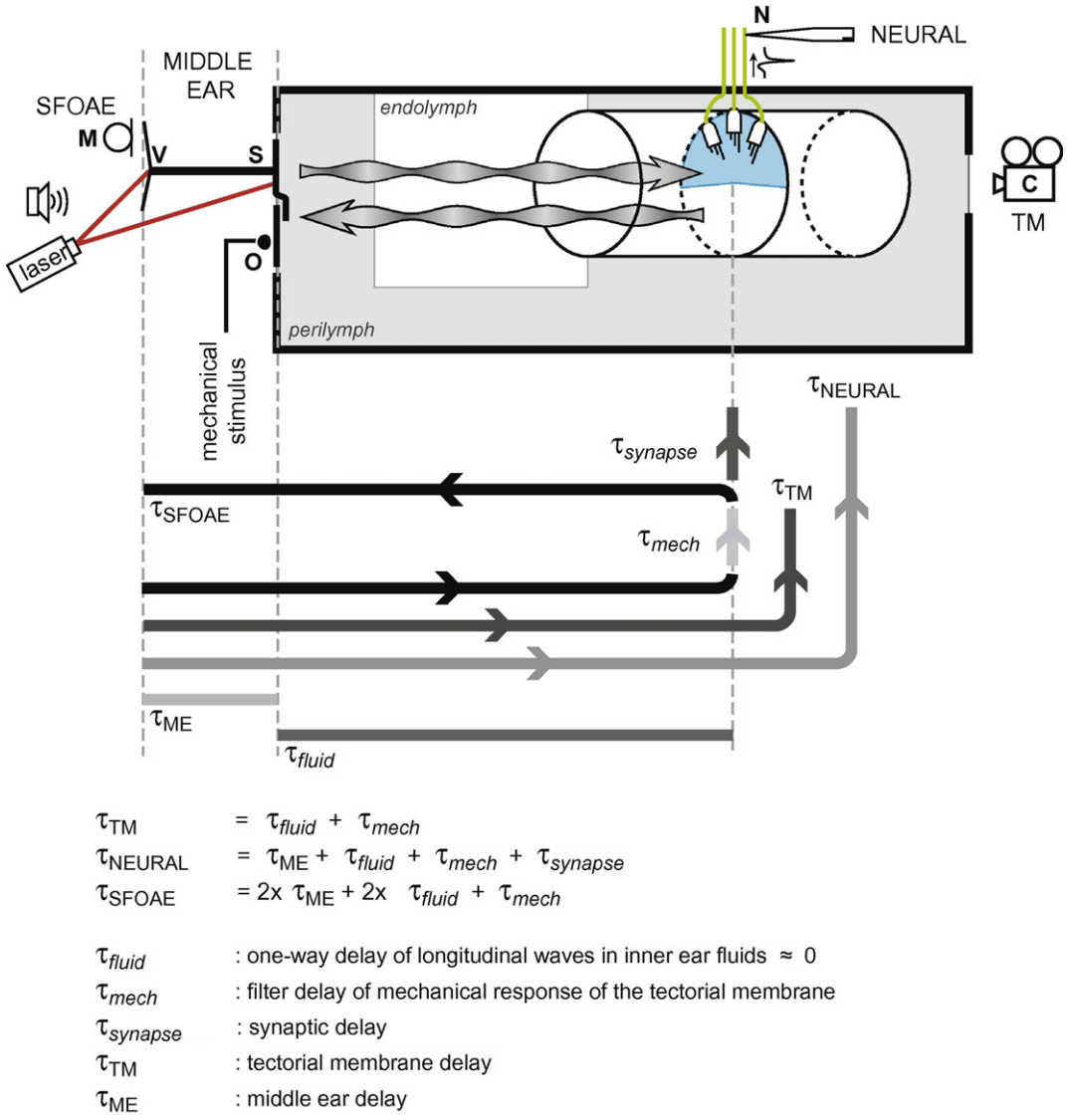

Fig. 8. Diagram illustrating the different recording sites and associated delays for the frog basilar papilla (BP). The stapes (S) connects to the otic capsule (grey rectangle) via the oval window, which also holds the operculum (O). Mechanical vibrations propagate through the inner ear fluids as longitudinal pressure waves (wavy arrows). Within the endolymphatic space (white rectangle), a rigid tubular structure contains the BP sensory epithelium. This is composed of hair cells in the wall of the tube, which are covered by the semicircular tectorial membrane (blue). Hair cells in the BP are only connected by afferent nerve fibers (green lines). The middle ear group delays from Fig. 2 were obtained by comparing the phase of the tympanic membrane velocity (V) with that of the microphone signal (M), or the stapes footplate velocity. For the tectorial membrane group delays (asterisk in Fig. 6), the phase of the mechanical stimulus of the piezo-electric stimulator on the operculum was compared to that of the tectorial membrane, as determined from movies obtained with a high-speed camera (C) focussed through the round window. Neural delays (closed symbols in Fig. 6) were calculated by comparing the acoustic stimulus (M) with the spike times of intracellular recordings from auditory fibers in the auditory nerve (N). The group delays for the SFOAE (circles in Fig. 6) were calculated by comparing the phase of the emissions with those of the stimulus tones, both calculated from the microphone signal (M). Note that τ-values with capital subscripts correspond to measured quantities.

via the basilar membrane. The delays of both waves would in this case contribute to the round-trip group delays of SFOAEs; in the forward direction in response to the original stimulus, and in the retrograde direction as the generated SFOAE (Shera and Guinan, 2003). Alternatively, only the forward wave could involve the basilar membrane, while the generated SFOAE may travel backward to the stapes as fluid compression sound waves, assumed to be essentially instantaneous. In this case, the round-trip would only include the delay of the forward travelling wave (Siegel et al., 2005; He et al., 2008). These consideration have led to estimates of the round-trip travel time ranging from 1× (Siegel et al., 2005; He et al., 2008), to between 1× and 2× (Shera et al., 2008), to 2× (Shera and Guinan, 2003) the forward delay.

Although the anatomy of the mammalian organ of Corti is very different to the frog's basilar papilla, the principal mechanisms of OAE generation may be similar. It is generally assumed that an SFOAE in the mammalian cochlea is generated in a region around the tonotopic place of its frequency. Thus, both in the mammalian cochlea and in the frog BP, the stimulus would travel to the location that is sensitive to its own frequency. In the cochlea, the high-order mechanical filter properties are determined by fluid coupling to adjacent cochlear locations (which also results in a travelling wave on the basilar membrane). In contrast, since the frog BP is essentially one filter with just one dominant tuning frequency (Ronken, 1990; Schoffelen et al., 2009) and no basilar membrane, there are no "adjacent" locations and no travelling waves to consider. Therefore the filtering properties (including the group delay) in the BP are only determined by local mechanisms. Thus, there is a difference in the mechanism by which the frequency selectivity comes about, but the principle of SFOAE generation may be the

Table 2
Group delays in the middle ear and the basilar papilla.

Delay from A to B		Reference
Sound pressure to tympanic membrane	0.53 (±0.07) ms	Mason and Narins, (personal communication)
Tympanic membrane to footplate/operculum**	0.170 (±0.005) ms	Mason and Narins (2002a)
Total middle ear delay (τ_{ME})	0.53 + 0.170 = 0.70 (±0.07) ms	
Operculum to tectorial membrane (τ_{TM})	0.60 (±0.08) ms	Schoffelen et al. (2009)
SFOAE delay (from stimulus sound pressure in front of the tympanic membrane to BP and back) (τ_{SFOAE})	2.0 (±0.1) ms*	Meenderink and Narins (2006)
Neural group delay from Wiener kernels (delay from sound pressure in front of the tympanic membrane to neuronal response) (τ_{NEURAL})	2.9 (±0.4) ms*	Van Dijk et al. (1997a,b)

* Mean and standard deviation obtained by averaging across the values in the interval 1700–2300 Hz, excluding one outlier near 0.1 ms in the SFOAE data.
** There is essentially no phase lag between the footplate and operculum response (Mason and Narins, 2002b).

same: an emission is generated at the tonotopic location after mechanical filtering by either the basilar membrane (cochlea) or tectorial membrane (BP). In the absence of the basilar membrane in the frog ear, anuran SFOAEs from the BP are likely to propagate via rapid, longitudinal sound waves within the inner ear fluids. We showed such a scheme to be consistent with measured group delays (Fig. 8). Interestingly, a similar mechanism has been proposed for reverse propagation of OAEs in the cochlea (Siegel et al., 2005; He et al., 2008), which would make the similarities between the anuran and mammalian SFOAEs even more complete.

A computation for the amphibian papilla similar to that presented for the BP cannot be performed, since there are no data available on the mechanical properties of the AP tectorial membrane. However, the differences between neural delays and SFOAE delays are similar in the AP and the BP frequency ranges (Fig. 6). This suggests a delay scheme that is similar to that in the BP (Fig. 8), and consistent with short delay estimates for the cochlea (Siegel et al., 2005; He et al., 2008).

Finally, we consider the total neural group delay τ_{NEURAL} and consider its correspondence with the collected group delays of subcomponents of the sound transmission path. The neural delay clearly decreases with increasing BEF (see Fig. 6). This delay is the sum of a number of components: (1) delay in the middle ear, (2) travel time in the inner ear fluids, which again will be neglected, (3) mechanical response of the tectorial membrane, (4) delay in the transduction and synapse, and finally (5) neuronal travel time. Hillery and Narins (1984) estimated the sum of components 1, 4 and 5 to be 2.0 ms in the frog *E. coqui*. Thus, with the middle ear component (1) being 0.70 (±0.07) ms (Fig. 1) in the bullfrog, and making the working assumption that the values would be similar between different frog species, the total synaptic and neural travel time delay (components 4 + 5) must be $\tau_{synapse} = 2.0-0.70$ (±0.07) = 1.30 (±0.07) ms. Ruggero and Rich (1987) estimated the equivalent delay to be 1 ms in mammals, a strikingly similar result. The mechanical response delay in the BP (component 3) is $\tau_{TM} = 0.60$ (±0.08) ms (Schoffelen et al., 2009). Thus, the total neural response group delay is predicted to be $\tau_{NEURAL,predicted} = \tau_{ME} + \tau_{TM} + \tau_{synapse} = 0.70$ (±0.07) + 0.60 (±0.08) + 1.30 = 2.60 (±0.11) ms. This corresponds well with the measured group delay of auditory neurons from the BP, $\tau_{NEURAL} = 2.9$ (±0.4) ms (Van Dijk et al., 1997a,b; see Table 2). Thus, the neural delay in the BP can be understood in terms of the delays of the middle ear, the tectorial membrane and the synapse.

In this paper, we have reviewed different types of data relating to the propagation and processing of auditory stimuli in anurans. These include middle ear mechanics, mechanical tuning of the tectorial membrane (in the BP), SFOAEs and neural responses. We have argued that the two auditory end-organs in the anuran ear (the amphibian papilla and the basilar papilla) should be considered as three, functionally distinct, systems: (1) the rostral portion of the AP, tuned to low frequencies, (2) the caudal part of the AP, most sensitive to the mid-frequency range, and (3) the basilar papilla, which is the tuned to the highest frequencies in the frog auditory range. None of these regions contains a basilar membrane which might support a travelling wave.

Despite the obvious anatomical differences between frog and mammalian inner ears, there are a number of intriguing functional similarities, which we have highlighted through our consideration of group delay measurements. In the BP, a comparison between the group delays of the different measures are remarkably consistent. We found that neural delays can be explained in terms of the delays associated with middle ear, tectorial membrane and synaptic transmission, and that round-trip SFOAE delays are the sum of the middle ear delays (both forward and reverse) and the tectorial membrane delay. This supports the contention that propagation within the inner ear fluids, in either direction, occurs via fast, longitudinal pressure waves. Further exploration of the frog inner ear, both anatomical and physiological, will doubtless help to expand our knowledge of this model of vertebrate auditory mechanics, which offers the dual benefits of morphological simplicity and physiological robustness, relative to the intractable and enigmatic mammalian cochlea.

Acknowledgements

We thank Mike Smotherman for discussions on the role of electrical tuning of hair cells in auditory frequency selectivity. We thank Hans Segenhout for discussions regarding the anatomy of the anuran inner ear. This work was supported by the Netherlands Organisation for Scientific Research (NWO) to P.v.D., R.L.M. and S.W.F.M., the Heinsius Houbolt Foundation to P.v.D. and R.L.M., and NIH Grant No. DC00222 to P.M.N.

References

Becker, R.P., Lombard, R.E., 1977. Structural correlates of function in the "operculars" muscle of amphibians. Cell Tissue Res. 175, 449–522.
Benedix Jr., J.H., Pedemonte, M., Velluti, R., Narins, P.M., 1994. Temperature dependence of two-tone rate suppression in the northern leopard frog, *Rana pipiens pipiens*. J. Acoust. Soc. Am. 96, 2738–2745.
Bergevin, C., Freeman, D.M., Saunders, J.C., Shera, C.A., 2008. Otoacoustic emissions in humans, birds, lizards, and frogs: evidence for multiple generation mechanisms. J. Comp. Physiol. A 194, 665–683.
Capranica, R.R., Moffat, A.J.M., 1980. Nonlinear properties of the peripheral auditory system of anurans. In: Popper, A.N., Fay, R.R. (Eds.), Comparative Studies of Hearing in Vertebrates. Springer, Berlin, pp. 139–165.
Dong, W., Olson, E.S., 2006. Middle ear forward and reverse transmission in gerbil. J. Neurophysiol. 95, 2951–2961.
Ehret, G., Capranica, R.R., 1980. Masking patterns and filter characteristics of auditory nerve fibers in the green treefrog (*Hyla cinerea*). J. Comp. Physiol. 141, 1–12.
Feng, A.S., Narins, P.M., Capranica, R.R., 1975. Three populations of primary auditory fibers in the bullfrog (*Rana catesbeiana*): their peripheral origins and frequency sensitivities. J. Comp. Physiol. 100, 221–229.
Fox, J.H., 1995. Morphological correlates of auditory sensitivity in anuran amphibians. Brain Behav. Evol. 45, 327–338.
Frishkopf, L.S., Capranica, R.R., Goldstein Jr., M.H., 1968. Neural coding in the bullfrog's auditory system – A teleological approach. Proc. IEEE 56, 969–980.
Frishkopf, L.S., Goldstein Jr., M.H., 1963. Responses to acoustic stimuli from single units in the eighth nerve of the bullfrog. J. Acoust. Soc. Am. 35, 1219–1228.
Gridi-Papp, M., Feng, A.S., Shen, J.-X., Yu, Z.-L., Narins, P.M., 2008. Active control of ultrasonic hearing in frogs. Proc. Natl. Acad. Sci. USA 105, 11013–11018.

He, W., Fridberger, A., Porsov, E., Grosh, K., Ren, T., 2008. Reverse wave propagation in the cochlea. Proc. Natl. Acad. Sci. USA 105, 2729–2733.
Hetherington, T.E., 1985. Role of the opercularis muscle in seismic sensitivity in the bullfrog *Rana catesbeiana*. J. Exp. Zool. 235, 27–43.
Hetherington, T.E., 1987. Physiological features of the opercularis muscle and their effects on vibration sensitivity in the bullfrog *Rana catesbeiana*. J. Exp. Biol., 189–204.
Hetherington, T.E., 1988. Biomechanics of vibration reception in the bullfrog, *Rana catesbeiana*. J. Cell. Comp. Physiol. A 163, 43–52.
Hetherington, T.E., 1994. The middle ear muscle of frogs does not modulate tympanic responses to sound. J. Acoust. Soc. Am. 95, 2122–2125.
Hetherington, T.E., Jaslow, A.P., Lombard, R.E., 1986. Comparative morphology of the amphibian opercularis system: I. General design features and functional interpretation. J. Morphol. 190, 43–61.
Narins, P.M., Hillery, C.M., 1983. Frequency coding in the inner ear of anuran amphibians. In: Klinke, R., Hartmann, R. (Eds.), Hearing-Physiological Bases and Psychophysics, vol. 183. Springer-Verlag, Heidelberg, pp. 70–76.
Hillery, C.M., Narins, P.M., 1984. Neurophysiological evidence for a traveling wave in the amphibian inner ear. Science 225, 1037–1039.
Jørgensen, M.B., Kanneworff, M., 1998. Middle ear transmission in the grass frog, *Rana temporaria*. J. Comp. Physiol. A 182, 59–64.
Kemp, D.T., 1978. Stimulated acoustic emissions from within the human auditory system. J. Acoust. Soc. Am. 64, 1386–1391.
Köppl, C., Manley, G.A., 1993. Spontaneous otoacoustic emissions in the bobtail lizard. I: General characteristics. Hear. Res. 71, 157–169.
Korenberg, M.J., 1973. Crosscorrelation analysis of neural cascades. In: Proceedings of the 10th Annual Rocky Mountain Bioengineering Symposium. Instrument Society of America, pp. 47–52.
Lewis, E.R., 1981. Suggested evolution of tonotopic organization in the frog amphibian papilla. Neurosci. Lett. 21, 131–136.
Lewis, E.R., Hecht, E., Narins, P.M., 1992. Diversity of form in the amphibian papilla of Puerto Rican frogs of the genus *Eleutherodactylus*. J. Comp. Physiol. 171, 469–476.
Lewis, E.R., Baird, R.A., Leverenz, E.L., Koyama, H., 1982. Inner ear: dye injection reveals peripheral origins of specific sensitivities. Science 215, 1641–1643.
Lewis, E.R., Leverenz, E.L., 1983. Morphological basis for tonotopy in the anuran amphibian papilla. Scan. Electron Microsc. 189–200.
Lewis, E.R., Leverenz, E.L., Koyama, H., 1982. The tonotopic organization of the bullfrog amphibian papilla, an auditory organ lacking a basilar membrane. J. Comp. Physiol. 145, 437–445.
Lewis, E.R., Narins, P.M., 1999. The acoustic periphery of amphibians: anatomy and physiology. In: Fay, R.R., Popper, A.N. (Eds.), Comparative Hearing: Fish and Amphibians. Springer-Verlag, New York, pp. 101–154.
Li, C.W., Lewis, E.R., 1974. Morphogenesis of auditory receptor epithelia in the bullfrog. Scan. Electron Microsc. 1974, 791–798.
Manley, G.A., Yates, G.K., Köppl, C., Johnstone, B.M., 1990. Peripheral auditory processing in the bobtail lizard *Tiliqua rugosa*. IV. phase locking of auditory-nerve fibers. J. Comp. Physiol. A 167, 129–138.
Manley, G.A., Van Dijk, P., 2008. Otoacoustic emissions in amphibians, lepidosaurs and archosaurs. In: Manley, G.A., Fay, R.R., Popper, A.N. (Eds.), Active Processes and Otoacoustic Emissions. Springer, pp. 211–260.
Mason, M.J., 2007. Pathways for sound transmission to the inner ear in amphibians. In: Narins, P.M., Feng, A.S., Fay, R.R., Popper, A.N. (Eds.), Hearing and Sound Communication in Amphibians, vol. 28. Springer, pp. 147–183.
Mason, M.J., Lin, C.C., Narins, P.M., 2003. Sex differences in the middle ear of the bullfrog (*Rana catesbeiana*). Brain Behav. Evol. 61, 91–101.
Mason, M.J., Narins, P.M., 2002. Vibrometric studies of the middle ear of the bullfrog *Rana catesbeiana* I. the extrastapes. J. Exp. Biol. 205, 3153–3165.
Mason, M.J., Narins, P.M., 2002. Vibrometric studies of the middle ear of the bullfrog *Rana catesbeiana* II. the operculum. J. Exp. Biol. 205, 3167–3176.
Meenderink, S.W.F., Kits, M., Narins, P.M., 2010. Frequency matching of vocalizations to inner-ear sensitivity along an altitudinal gradient in the coqui frog. Biol. Lett. 6, 278–281.
Meenderink, S.W.F., Narins, P.M., 2006. Stimulus frequency otoacoustic emissions in the northern leopard frog, *Rana pipiens pipiens*: Implications for inner ear mechanics. Hear. Res. 220, 67–75.
Meenderink, S.W.F., Narins, P.M., 2007. Suppression of distortion product otoacoustic emissions in the anuran ear. J. Acoust. Soc. Am. 121, 344–351.
Meenderink, S.W.F., Van Dijk, P., 2005. Detailed f1, f2 area study of distortion product otoacoustic emissions in the frog. JARO 6, 37–47.
Meenderink, S.W.F., Van Dijk, P., 2006. Temperature dependence of anuran distortion product otoacoustic emissions. J. Assoc. Res. Otolaryngol. 7, 246–252.
Narins, P.M., Capranica, R.R., 1980. Neural adaptations for processing the two-tone call of the Puerto Rican treefrog, *Eleutherodactylus coqui*. Brain Behav. Evol. 17, 48–66.
Palmer, A.R., Wilson, J., 1982. Spontaneous and evoked otoacoustic emissions in the frog *Rana esculenta*. J. Physiol. 324, 66P.
Pitchford, S., Ashmore, J.F., 1987. An electrical resonance in hair cells of the amphibian papilla of the frog *Rana temporaria*. Hear. Res. 27, 75–83.
Purgue, A.P., Narins, P.M., 2000. Mechanics of the inner ear of the bullfrog (*Rana catesbeiana*): the contact membranes and the periotic canal. J. Comp. Physol. A 186, 481–488.
Purgue, A.P., Narins, P.M., 2000. A model for energy flow in the inner ear of the bullfrog (*Rana catesbeiana*). J. Comp. Physiol. A 186, 489–495.
Recio-Spinoso, A., Temchin, A.N., van Dijk, P., Fan, Y.-H., Ruggero, M.A., 2005. Wiener-kernel analysis of responses to noise of chinchilla auditory-nerve fibers. J. Neurophysiol. 93, 3615–3634.
Ronken, D.A., 1990. Basic properties of auditory-nerve responses from a 'simple' ear: the basilar papilla of the frog. Hear. Res. 47, 63–82.
Ronken, D.A., 1991. Spike discharge properties that are related to the characteristic frequency of single units in the frog auditory nerve. J. Acoust. Soc. Am. 90, 2428–2440.
Ruggero, M.A., Rich, N.C., 1987. Timing of spike initiation in cochlear afferents: dependence on site of innervation. J. Neurophysiol. 2, 379–403.
Schetzen, M., 1989. The Volterra and Wiener Theories of Nonlinear Systems. Krieger, Malabar, Florida.
Schoffelen, R.L.M., 2009. Auditory Mechanics of the Frog Basilar Papilla. PhD thesis, University of Groningen.
Schoffelen, R.L.M., Segenhout, J.M., Van Dijk, P., 2008. Mechanics of the exceptional anuran ear. J. Comp. Physiol. A 194, 417–428.
Schoffelen, R.L.M., Segenhout, J.M., Van Dijk, P., 2009. Tuning of the tectorial membrane in the basilar papilla of the northern leopard frog. J. Assoc. Res. Otolaryngol. 10, 309–320.
Shera, C.A., Guinan, J.J., 2003. Stimulus-frequency-emission group delay: a test of coherent reflection and a window on cochlear tuning. J. Acoust. Soc Am. 113, 2762–2772.
Shera, C.A., Tubis, A., Talmadge, C.L., 2008. Testing coherent reflection in chinchilla auditory-nerve responses predict stimulus-frequency emissions. J. Acoust. Soc. Am. 124, 381–395.
Shofner, W.P., Feng, A.S., 1981. Post-metamorphic development of the frequency selectivity and sensitivity of the peripheral auditory system of the bullfrog, *Rana catesbeiana*. J. Exp. Biol. 93, 181–196.
Siegel, J.H., Cerka, A.J., Recio-Spinoso, A., Temchin, A.N., van Dijk, P., Ruggero, M.A., 2005. Delays of stimulus-frequency otoacoustic emissions and cochlear vibrations contradict the theory of coherent reflection filtering. J. Acoust. Soc. Am. 118, 2434–2443.
Smotherman, M.S., Narins, P.M., 1999. The electrical properties of auditory hair cells in the frog amphibian papilla. J. Neurosci. 19, 5275–5292.
Smotherman, M.S., Narins, P.M., 2000. Hair cells, hearing and hopping: a field guide to hair cell physiology in the frog. J. Exp. Biol. 203, 2237–2246.
Talmadge, C., Long, G., Murphy, W., Tubis, A., 1993. New off-line method for detecting spontaneous otoacoustic emissions in human subjects. Hear. Res. 71, 170–182.
Van Dijk, P., Manley, G.A., 2001. Distortion product otoacoustic emissions in the tree frog *Hyla cinerea*. Hear. Res. 153, 14–22.
Van Dijk, P., Narins, P.M., Mason, M.J., 2003. Physiological vulnerability of distortion product otoacoustic emissions from the amphibian ear. J. Acoust. Soc Am. 114, 2044–2048.
Van Dijk, P., Narins, P.M., Wang, J., 1996. Spontaneous otoacoustic emissions in seven frog species. Hear. Res. 101, 102–112.
Van Dijk, P., Wit, H.P., Segenhout, J.M., 1989. Spontaneous otoacoustic emissions in the European edible frog (*Rana esculenta*): spectral details and temperature dependence. Hear. Res. 42, 273–282.
Van Dijk, P., Wit, H.P., Segenhout, J.M., 1997. Dissecting the frog inner ear with Gaussian noise: I. application of high-order Wiener-kernel analysis. Hear. Res. 114, 229–242.
Van Dijk, P., Wit, H.P., Segenhout, J.M., 1997. Dissecting the frog inner ear with Gaussian noise: II. temperature dependence of inner ear response. Hear. Res. 114, 243–251.
Van Dijk, P., Wit, H.P., Segenhout, J.M., Tubis, A., 1994. Wiener kernel analysis of inner ear function in the American bullfrog. J. Acoust. Soc. Am. 95, 904–919.
Wever, E.G., 1973. The ear and hearing in the frog, *Rana pipiens*. J. Morphol. 141, 461–478.
Wever, E.G., 1985. The Amphibian Ear. Princeton University Press, Princeton, New Jersey.
Yamada, W.M., Lewis, E.R., 1999. Predicting the temporal responses of non-phase-locking bullfrog auditory units to complex acoustic waveforms. Hear. Res. 130, 155–170.